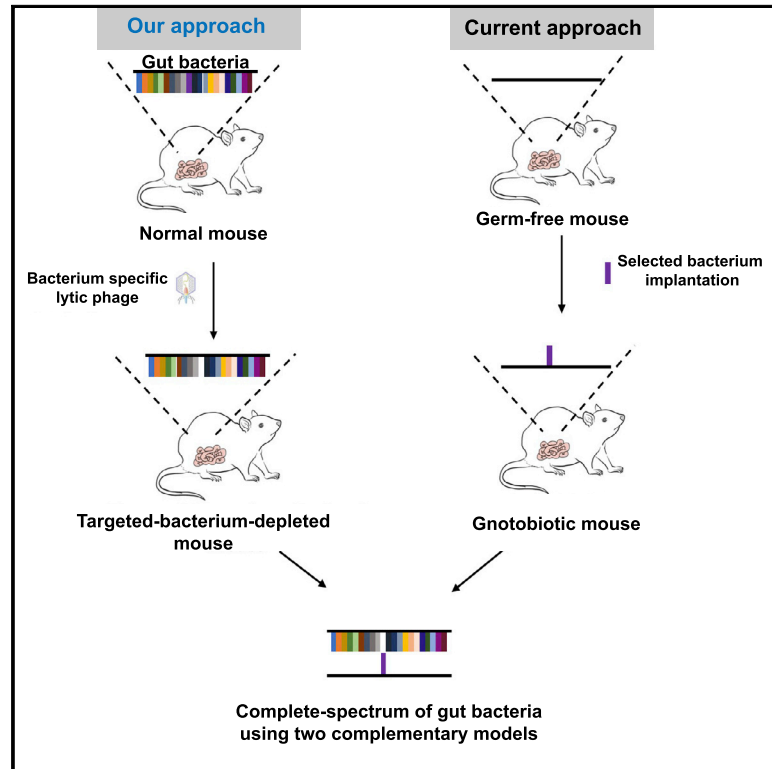


# Bacteriophages allow selective depletion of gut bacteria to produce a targeted-bacterium-depleted mouse model

## Graphical abstract



## Authors

Yanqing Li, Feng Zhu, Yan Li, ...,  
Yawen Wang, Xiancang Ma, Bing Liu

## Correspondence

wangyw1269@xjtu.edu.cn (Y.W.),  
maxiancang@163.com (X.M.),  
bliu2018@xjtu.edu.cn (B.L.)

## In brief

Li et al. propose a targeted-bacterium-depleted (TBD) mouse model using host-specific bacteriophages to selectively deplete targeted gut bacterium. They demonstrate that *Escherichia coli*-depleted mice acquire traits resembling fearlessness, demonstrating the potential utility of this model for microbiota-gut-brain axis studies.

## Highlights

- We make a targeted-bacterium-depleted (TBD) mouse model using bacteriophages
- Bacteriophages with a narrow host range allow depletion of specific gut bacteria
- The TBD mouse model complements gnotobiotic mouse models
- *Escherichia coli*-depleted mice acquire behaviors resembling fearlessness



## Article

# Bacteriophages allow selective depletion of gut bacteria to produce a targeted-bacterium-depleted mouse model

Yanqing Li,<sup>1,9</sup> Feng Zhu,<sup>2,3,4,9</sup> Yan Li,<sup>3,9</sup> Shunli Pan,<sup>1</sup> Hongliang Wang,<sup>5</sup> Zai Yang,<sup>2</sup> Zhihao Wang,<sup>1</sup> Zhenyu Hu,<sup>1</sup> Jianfeng Yu,<sup>6</sup> Joseph D. Barritt,<sup>6</sup> Tianhui Li,<sup>7</sup> Xi Liu,<sup>8</sup> Yawen Wang,<sup>1,\*</sup> Xiancang Ma,<sup>2,3,\*</sup> and Bing Liu<sup>1,6,10,\*</sup>

<sup>1</sup>BioBank, The First Affiliated Hospital of Xi'an Jiaotong University, Shaanxi 710061, China

<sup>2</sup>Department of Psychiatry, The First Affiliated Hospital of Xi'an Jiaotong University, Shaanxi 710061, China

<sup>3</sup>Center for Brain Research, The First Affiliated Hospital of Xi'an Jiaotong University, Shaanxi 710061, China

<sup>4</sup>Center for Translational Medicine, The First Affiliated Hospital of Xi'an Jiaotong University, Shaanxi 710061, China

<sup>5</sup>Department of Pathogen Biology and Immunology, Xi'an Jiaotong University Health Science Center, Xi'an, Shaanxi 710061, China

<sup>6</sup>Department of Life Sciences, Imperial College London, London SW7 2AZ, UK

<sup>7</sup>Department of Biomedical Engineering, School of Life Science and Technology, Xi'an Jiaotong University, Xi'an, Shaanxi 710061, China

<sup>8</sup>Department of Pathology, First Affiliated Hospital of Xi'an Jiaotong University, Xi'an, Shaanxi 710061, China

<sup>9</sup>These authors contributed equally

<sup>10</sup>Lead contact

\*Correspondence: wangyw1269@xjtu.edu.cn (Y.W.), maxiancang@163.com (X.M.), bliu2018@xjtu.edu.cn (B.L.)

<https://doi.org/10.1016/j.crmeth.2022.100324>

**MOTIVATION** In cell biology, gene overexpression and knockout/knockdown techniques are commonly used in pairs to study a selected gene. In gut microbiota studies, bacterium implantation and gnotobiotic animal models are used to investigate bacterium of interest, resembling gene overexpression in wild-type and modified cell strains, respectively. Yet, there is still no standard protocol to knock out/knock down bacteria in gut microbiota studies. We therefore developed a gut bacteria knockdown technique using bacteriophages, resembling gene knockdown methods. The resulted targeted-bacterium-depleted (TBD) animal model allows us to study the function of targeted bacterium in complement with implantation-based models.

## SUMMARY

The gut microbiome is essential for human health. Mouse microbiota models, including gnotobiotic mice, are the most prominent tools to elucidate the functions of gut bacteria. Here, we propose a targeted-bacterium-depleted (TBD) model using lytic bacteriophage to selectively deplete gut bacterium of healthy or otherwise defined mice. These phage-treated animals should have a near-complete spectrum of gut bacteria except for the depleted bacterium. To prove the concept, we employed *Escherichia coli*-specific phage T7 to repress *E. coli* in the healthy mice. Our results showed that the *E. coli*-depleted mice exhibited bravery-like behaviors, correlated to the presence of *E. coli* rather than the equilibrium among gut bacteria. Thus, we demonstrate that the TBD model is a powerful tool to elucidate the function of a specific bacterial species within a near-intact gut microbiota environment and complements gnotobiotic mice models.

## INTRODUCTION

The gut is the largest microbiota reservoir in the human body and is inhabited by a range of bacteria, eukaryotes, and viruses (Kho and Lal, 2018). With approximately  $10^{14}$  cells in population (Sender et al., 2016), the diversity and interactions of gut bacteria substantially influence host metabolism, hence its link to many aspects of human health (Quigley, 2013). For example, the gut microbiota regulates the maturation of host immune responses,

as well as diseases including cancers that are related to altered microbiota composition (Visconti et al., 2019; Zitvogel et al., 2015). In addition, the administration of drugs often has an impact on gut microbiota. Drug-bacteria interactions have a profound impact on some therapeutics used to treat mental health conditions like schizophrenia (Walsh et al., 2018; Weersma et al., 2020).

The microbiota-gut-brain axis (MGB) is a classic example of microbiota-host interactions (Carabotti et al., 2015). Expanded



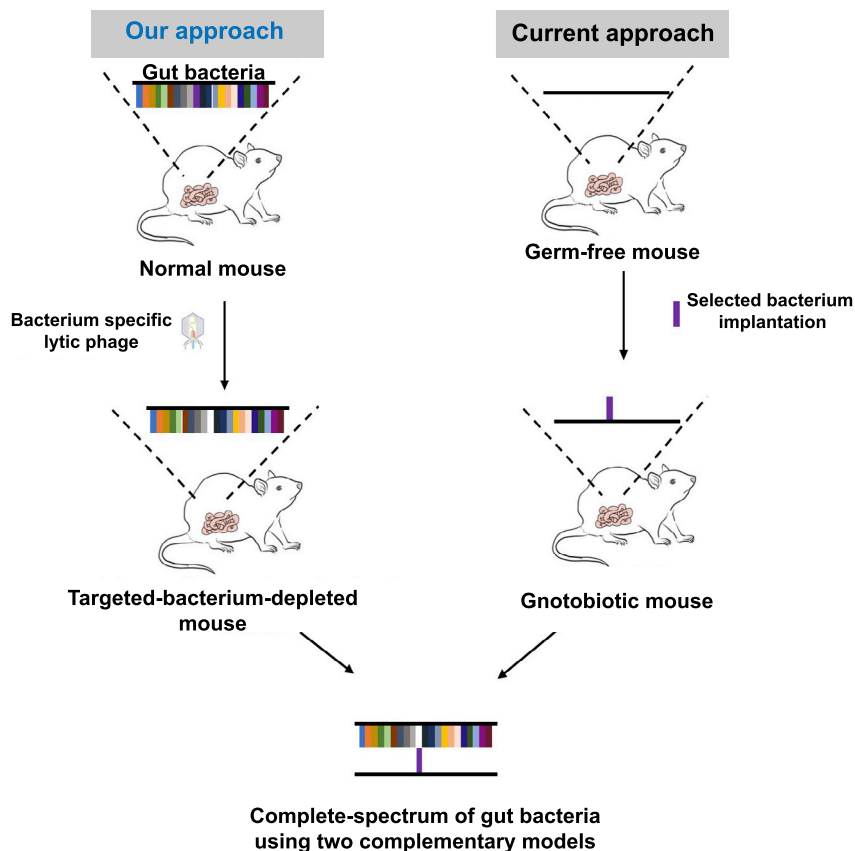


**Figure 1. Targeted-bacterium-depleted (TBD) model compared with gnotobiotic model**

TBD model using lytic bacteriophage to repress level of targeted bacteria provides a complementary approach to the gnotobiotic mouse model.

free (SPF) mice (Kennedy et al., 2018). These animal models have their own advantages: the antibiotic-treated mouse model is simple to study but is incapable of assessing the impact of individual bacterial strains due to broad specificity. While the gnotobiotic mouse model, using germ-free mice that were inoculated with selected microbes, is the gold standard to study specific strains, its physiological impact may not be representative in the natural environment. In addition, studies using gnotobiotic models are time consuming and expensive (Umesaki, 2014).

Here, we propose a new animal model that combines the benefits of the gnotobiotic mouse model for bacterial strain precision and the ease to establish by just using the normal mouse. By using lytic bacteriophage, a specific gut bacterium can be targeted for depletion in the animal model. To demonstrate the feasibility of this hypothesis, we chose to deplete *E. coli* from the gut of healthy mice using *E. coli*-specific

from the gut-brain axis (GBA), which describes the bidirectional communication between the brain and the enteric nervous system, MGB describes the relationship between the gut microbiota and the central nervous system (Petra et al., 2015). For example, gut microbes can produce neuroactive molecules that signal between the enteric nervous system and the brain via the vagus nerve (Galland, 2014). The composition of microbiota can also be modulated via the intestinal epithelial cells through the hypothalamic-pituitary-adrenal (HPA) axis during stressful conditions (Stephens and Wand, 2012). The abundance of some gut bacteria is correlated with mental health conditions, defined as the psychobiome (Matarazzo et al., 2018). For example, schizophrenia-like behaviors can be induced by *Streptococcus vestibularis* in the gut (Zhu et al., 2020), and patients with depression often have reduced levels of *Coprococcus* and *Dialister* (Valles-Colomer et al., 2019).

*E. coli*, which constitutes 0.1%–5% of the gut microbiota, is a well-characterized model organism with which to study the MGB (Arumugam et al., 2011; Knight and Girling, 2003). While it produces vitamin K and B12 that are essential for the mammalian host to function, it may also induce psychiatric symptoms in patients (Kleimann et al., 2014). Furthermore, healthy mice with induced anxiety-like behaviors have elevated levels of gut *E. coli* (Jang et al., 2018). Much of our current understanding of the MGB was determined using artificial animal models with antimicrobial treatment including germ-free and specific-pathogen-

bacteriophage T7 and quantified the effects with both molecular and phenotypic analyses, as summarized in Figure 1. To our surprise, these *E. coli* targeted-bacterium-depleted (TBD) mice demonstrated behavioral changes that resemble previously published effects of anxiolytic and antidepressant therapeutics (Burakas et al., 2017; Shi et al., 2020; Wang et al., 2019). These otherwise healthy animals acquired a “brave” personality compared with the control group, without being hyperactive. Thus, we show that the TBD mice model offers a complementary route to validate data from gnotobiotic models and could be used to study a wide range of gut bacteria by carefully selecting their bacteriophages.

## RESULTS AND DISCUSSION

### T7 phage administration had no noticeable effect on the physical condition of the mice

To validate our model, T7 phage, which targets most *E. coli* strains, was used to limit the complexity that a phage cocktail may cause. We set up four parallel groups in which mice were intragastrically administered T7 at  $10^6$  plaque-forming unit (PFU)/mL ( $T7^L$ ), T7 at  $10^{11}$  PFU/mL ( $T7^H$ ), deactivated (autoclaved) T7 at  $10^{11}$  PFU/mL ( $dT7^H$ ), and water, respectively. Various vital signs were measured, stool samples were collected on a daily basis, and a collection of behavioral tests were carried out at regular intervals (Figure 2A). As anticipated, T7 phage did not have

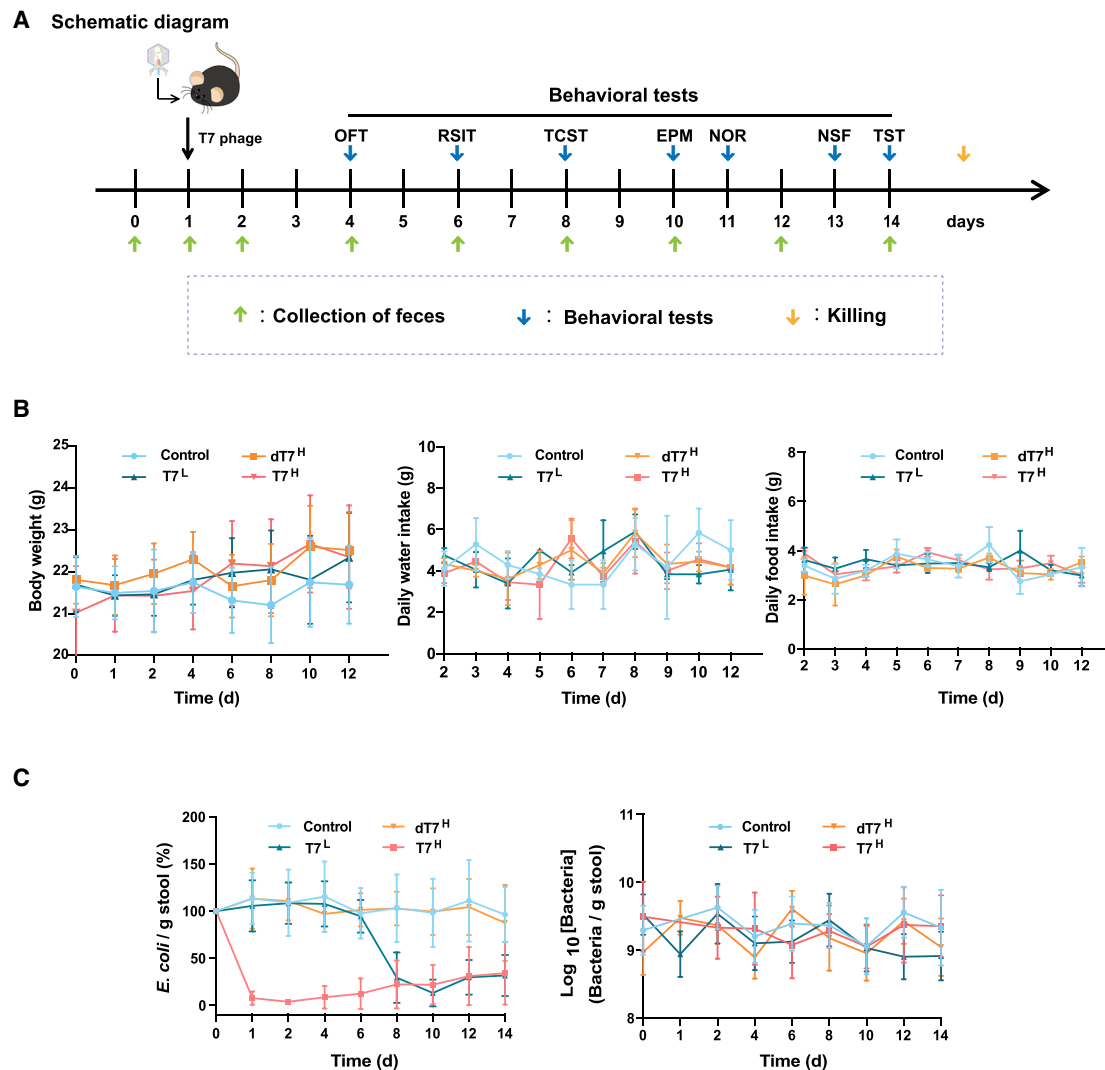


**Figure 2. T7 phage represses the *E. coli* level without affecting the physical conditions and the overall population of gut bacteria**

(A) The schematic diagram of the time frame and the behavioral tests employed in this study (n = 12 for each group). OFT, open-field test; RSIT, reciprocal social interaction test; TCST, three-chamber sociability test; EPM, elevated plus-maze test; NOR, novel object recognition test; NSF, novelty-suppressed feeding test; TST, tail suspension test.

(B) Physical conditions: body weight (left, mean ± SD), daily water intake (middle, mean ± SD), and daily food intake (right, mean ± SD) measured for each group (n = 12) at different times.

(C) The level of *E. coli* (left, mean ± SD) and the level of total bacteria (right, mean ± SD) quantified by qPCR over time (n = 12 for each group).

noticeable influence on the physical condition of the mice based on their daily food intake and body weight (Figure 2B).

### T7 phage selectively depleted *E. coli* but did not affect the overall gut bacterial population

We used qPCR to quantify the population of *E. coli* and total gut bacteria to track the dynamic changes after phage administration. Over the course of 14 days, the overall population of gut bacteria in all groups did not show significant perturbation. In contrast, the *E. coli* population in the T7<sup>H</sup> group immediately reduced to ~10% and gradually recovered to ~25% by day 14 compared with control, presumably due to its acquired resistance to phage. Furthermore, there was a delayed onset in

the drop of the *E. coli* population in the T7<sup>L</sup> group, where the decline only started after day 6 (Figure 2C) and reached the same level as T7<sup>H</sup> on day 8. To verify the correlation between *E. coli* and the phage, we compared the populations of T7 and *E. coli* in the T7-treated groups using qPCR. In the dT7<sup>H</sup> group, the trackable T7 DNA decreased readily, while *E. coli* remained undisturbed (Figure S1A). In contrast, the *E. coli* population dropped significantly after T7 administration in the T7<sup>H</sup> group, while the level of T7 was maintained at a very high level throughout (Figure S1B). In the T7<sup>L</sup> group, the *E. coli* population only started declining after day 6, while the level of T7 was maintained at the moderate level after the drop of *E. coli* (Figure S1C). In summary, the general trend for the *E. coli*

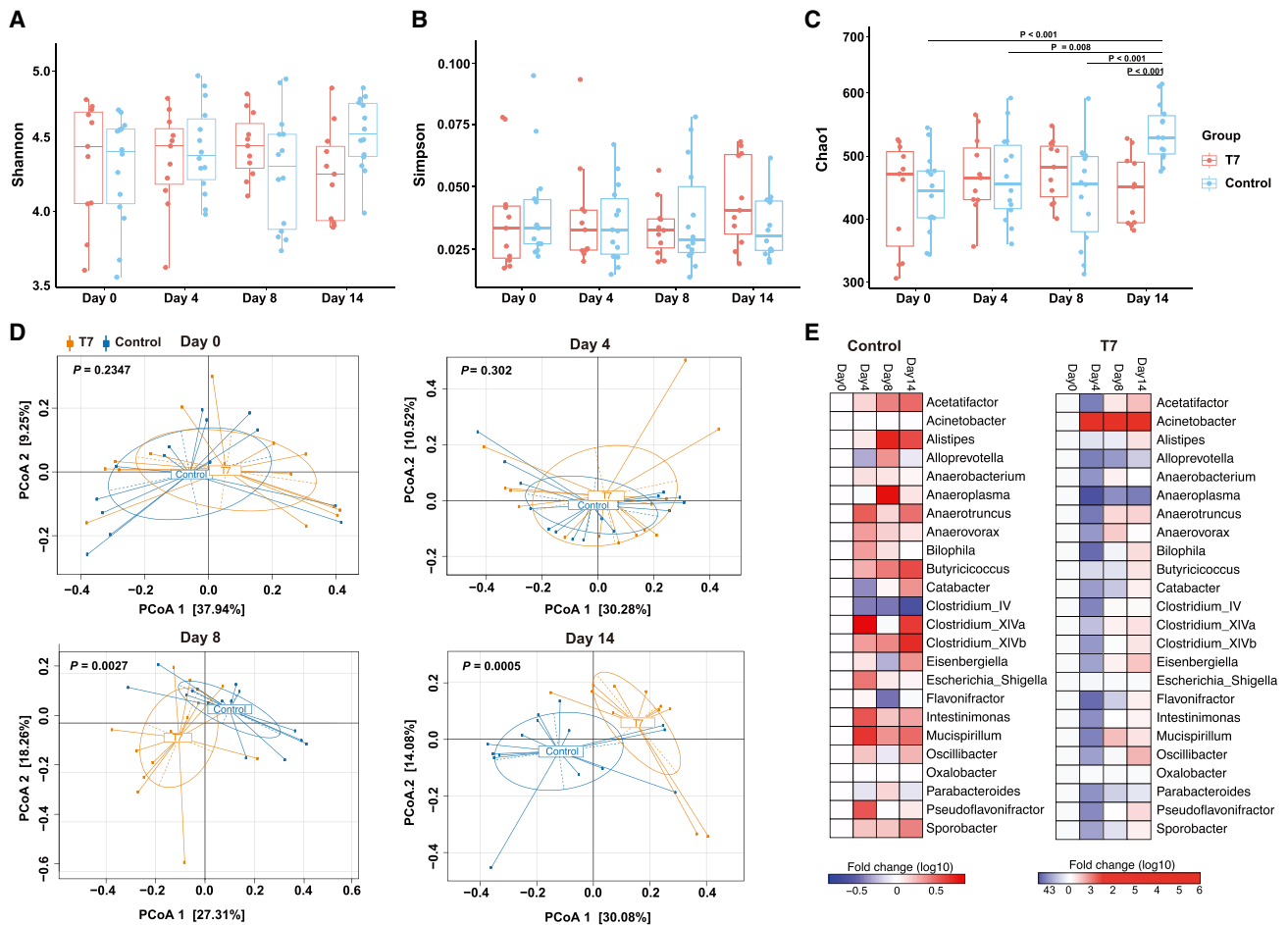


**Figure 3. Depletion of *E. coli* induced dynamic changes in gut microbiota**

Gut microbiota were profiled using absolute quantification of 16S rRNA amplicon sequencing at baseline (day 0) and 4, 8, and 14 days after a gavage of killed (control group) or T7 phage (T7<sup>+</sup>).

(A–C) Shannon, Simpson, and Chao1 indices of alpha diversity of gut microbiota calculated by amplicon sequence variant at four time points in each group of mice (n = 12 for each group; data displayed as mean ± SD). p values for the comparisons of alpha diversity between two groups of mice at same time point or between different time points within same mice group are calculated via repeated-measures ANOVA.

(D) Principal-coordinate analysis (PCoA) based on Bray-Curtis metrics was conducted at four time points in each group of mice (n = 12 for each group). p values for the comparisons of overall microbial community composition between two groups of mice at same time point are calculated by permutational multivariate ANOVA using distance matrices.

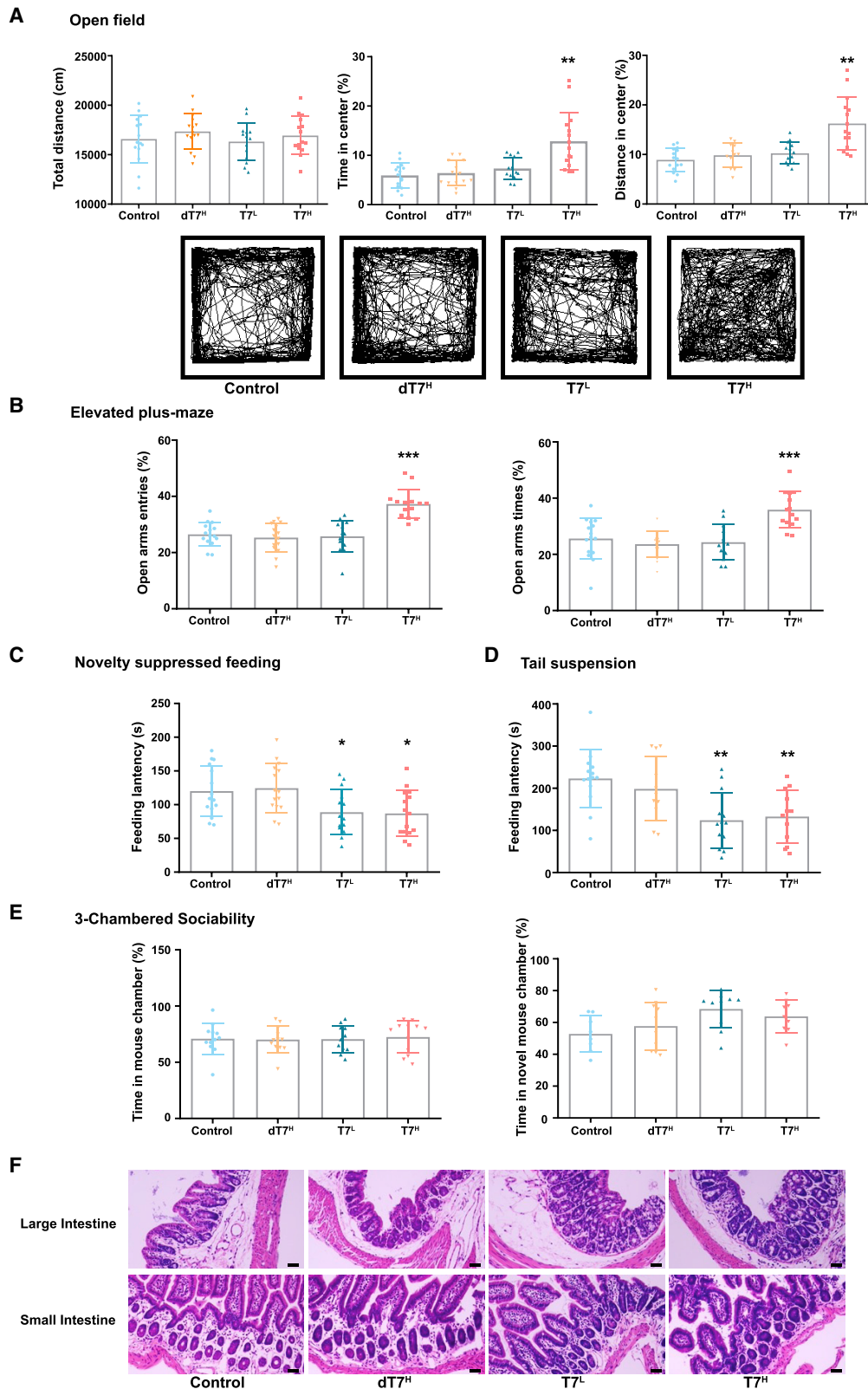
(E) The abundance changes of 24 bacterial genera that are regulated by T7 phage and significantly change over time are shown in two heatmaps: left for control group, and right for T7 group (n = 12 for each group). Four blocks for each bacterium indicate four time points. The color represents the change fold of absolute abundance in contrast to that at baseline.

population agreed with a previous study using phages in a gnotobiotic-based mice model (Hsu et al., 2019).

### ***E. coli* depletion caused a decrease in species representation in the gut microbiota**

To investigate the cascading effect of *E. coli* diminishment, we used 16S rRNA gene amplicon sequencing and internal references of specific DNA fragments to quantify the absolute abundance of the microbial taxon to assess the dynamic changes in gut microbiota. Fecal microbiota compositions were investigated at four time points, i.e., the baseline and 4, 8, and 14 days after a gavage of T7 phage administration. There were statistically significant interaction effects of time × T7 phage

on bacterial community richness in gut (Chao1 index:  $F_{(3, 69)} = 5.8$ ,  $p = 0.001$ ) but with no effects on Shannon ( $F_{(3, 69)} = 2.41$ ,  $p = 0.075$ ) and Simpson diversity indices ( $F_{(3, 69)} = 0.84$ ,  $p = 0.475$ , repeated-measures ANOVA; Figures 3A–3C; Table S1). Similar bacterial richness existed between two groups of mice at the first three time points ( $F_{(1,23)} = 0–1.66$ , all  $p > 0.211$ ), whereas decreased bacterial richness was presented in the gut of *E. coli*-depleted mice relative to the control mice 14 days after a gavage of T7 phage ( $F_{(1,23)} = 20.71$ ,  $p = 0.0001$ ; Figure 3C). With respect to beta diversity, both time and T7 phage exerted significant effects on overall microbial composition (Figures 3D and S2; Table S2). Along with T7 phage treatment, beta diversity of gut microbiota in *E. coli*-depleted mice



(legend on next page)



gradually decreased (adjusted p value [ $p_{\text{adj}}$ ] = 0.0002), and their beta diversity elevated on day 8 ( $p_{\text{adj}}$  = 0.0054) but decreased on day 14 ( $p_{\text{adj}}$  = 0.002) after phage gavage relative to the control mice (permutational multivariate ANOVA [PERMANOVA] for Bray–Crutis distance; Table S2; Figure S2). Bacterial taxa did not significantly vary between *E. coli*-depleted mice and control mice until post-phage gavage day 8 (Wilcoxon rank test:  $p_{\text{adj}}$  > 0.1). The absolute abundances of 25 and 31 intestinal bacterial genera in *E. coli*-depleted mice diverged from the control mice on post-phage gavage days 4 and 14, respectively (Wilcoxon rank test:  $p_{\text{adj}}$  < 0.1; Table S3). Moreover, the abundance of 24 intestinal bacterial genera displayed obvious longitudinal changes (interaction effects of time and T7 phage:  $F_{(1,23)} = 3.202\text{--}112.513$ , all  $p < 0.029$ ; Table S4), whereas the patterns of longitudinal trajectories of altered microbiota were different between the two groups (Figure 3E).

### ***E. coli*-depleted mice exhibited abnormal behaviors**

To correlate the impact of gut *E. coli* on the host, we performed seven behavioral tests covering both mental states and sociability, in which five tests have shown statistically significant differences in the T7<sup>H</sup> group compared with the control group. In an open-field test (OFT), while the total distances for each group showed no difference, which suggests a similar basal locomotor activity across the groups, the T7<sup>H</sup> group spent more time in the brightly lit open areas and displayed a behavioral pattern similar to the administration of anxiolytics (Seibenhener and Wooten, 2015) (Figure 4A). In the elevated plus-maze (EPM) test, mice in the T7<sup>H</sup> group entered opened arms more frequently and persisted longer, which demonstrates a similar pattern to previously reported anxiolytic mice (Walf and Frye, 2007) (Figure 4B). In a novelty-suppressed feeding (NSF) experiment, the feeding latency for mice from both T7<sup>H</sup> and T7<sup>L</sup> groups was reduced, as the test was performed on day 8 when the *E. coli* population of T7<sup>L</sup> was equivalent to the T7<sup>H</sup> group (Figure 4C). As NSF is sensitive to acute administration of anxiolytics and chronic antidepressant treatment but not acute antidepressants, both T7-treated animal groups displayed behaviors resembling that of previously described administration of anxiolytics (Ramaker and Dulawa, 2017). During the tail suspension test (TST), immobility time for mice from both T7<sup>H</sup> and T7<sup>L</sup> was significantly shorter than the control groups (Figure 4D). Since TST is generally used for assessing antidepressant activity, phage T7 acted as an effective antidepressant but not anxiolytic (Cryan et al.,

2005). In contrast, there were no differences between the groups' general sociability and interest in social novelty. These metrics were assessed by the three-chambered social test (TCST) (Kaidanovich-Beilin et al., 2011), autism-related behavioral deficits were assessed by reciprocal social interaction test (RSIT) (Kim et al., 2019), and learning and memory in mice were evaluated by novel object recognition (NOR) test (Lueptow, 2017), which suggested that the general sociability and memory of the mice were not affected by the phage (Figures 4E and S3A–S3C). Notably, the *E. coli* population in the T7<sup>L</sup> group dropped to T7<sup>H</sup> levels on day 8, and it was this exact time point when the group started to show behavior abnormalities similar to that of the T7<sup>H</sup> group. Thus, the results from two experimental groups demonstrated, in parallel, that the behavioral disturbances in the mice were directly related to the *E. coli* population rather than the cascading effect on global gut microbiota.

### **No pathological abnormality found on the major organs of the phage-treated mice**

Anatomically, the epithelium of the small intestine and large intestine displayed reactive hyperplasia with preservation of the normal glandular architecture and nuclear polarity (Figure 4F), and the cells showed a mildly increased nuclear-to-cytoplasmic ratio, slightly enlarged nuclei, hyperchromasia, and an increased mitotic rate, while marked pleomorphism and atypical mitoses were absent. Moreover, there was no observable abnormality in other major organs, i.e., the pathologic morphology of brain, heart, lung, liver, spleen, and kidney displayed no differences among all groups, suggesting that physiological health of the host is unlikely linked to the behavioral alterations (Figure S4).

### **Behavioral restoration is correlated with the recovery of *E. coli* population**

As the *E. coli* gradually restored to 25% occupancy of the pre-T7 level on day 14, it would be important to determine if the bacterium could fully recover to normal after the phage intervention (Figure 2C). We repeated the experiments with the control and T7<sup>H</sup> groups and traced the fecal *E. coli* level using qPCR. The *E. coli* level on day 16 was approximately 30% of the control, similar to the level that was observed on day 14 in the previous experiment (Figure 5A). The bacterial level continued to recover and restored to pre-phage treatment levels at approximately day 24. To confirm that the behavioral abnormalities are due to the *E. coli* depletion, we also performed a rescue experiment by gavaging *E. coli* to

#### **Figure 4. *E. coli* depletion exhibited combined anxiolytics-treated behavior patterns in mice**

- (A) The open-field test for each group (n = 12; data displayed as mean ± SD). The total distance travelled by the mice is measured (top left), the percentage of time spent in the center of the device (top middle) and the percentage of distance in the center of the device are calculated (top right), and the tracing of mouse movement during the 30 min test period is also recorded (bottom). \*\*p < 0.01, T7<sup>H</sup> versus control group.
- (B) The elevated plus-maze test for each group (n = 12; data displayed as mean ± SD). The percentage of time spent in the open arms and the percentage of entries to the open arms of the device are calculated. \*\*\*p < 0.001, T7<sup>H</sup> versus control group.
- (C) The novelty suppressed feeding test where the feeding latency was measured (n = 12; data displayed as mean ± SD). \*p < 0.05, T7<sup>L</sup> and T7<sup>H</sup> versus control group.
- (D) The tail suspension test where the immobility time was measured (n = 12; data displayed as mean ± SD). \*\*p < 0.01, T7<sup>L</sup> and T7<sup>H</sup> versus control group.
- (E) Three-chambered sociability test where the percentage of time spent in either mouse chamber or novel mouse chamber was calculated (n = 12; data displayed as mean ± SD).
- (F) Pathologic morphology of the epithelium cell of small intestine and large intestine of each group exhibited reactive hyperplasia with preservation of the normal glandular architecture and nuclear polarity across the groups. The cells show mild increased nuclear-to-cytoplasmic ratio, slightly enlarged nuclei, hyperchromasia, and an increased mitotic rate, while marked pleomorphism and atypical mitoses were absent. Scale bars, 0.5 mm.

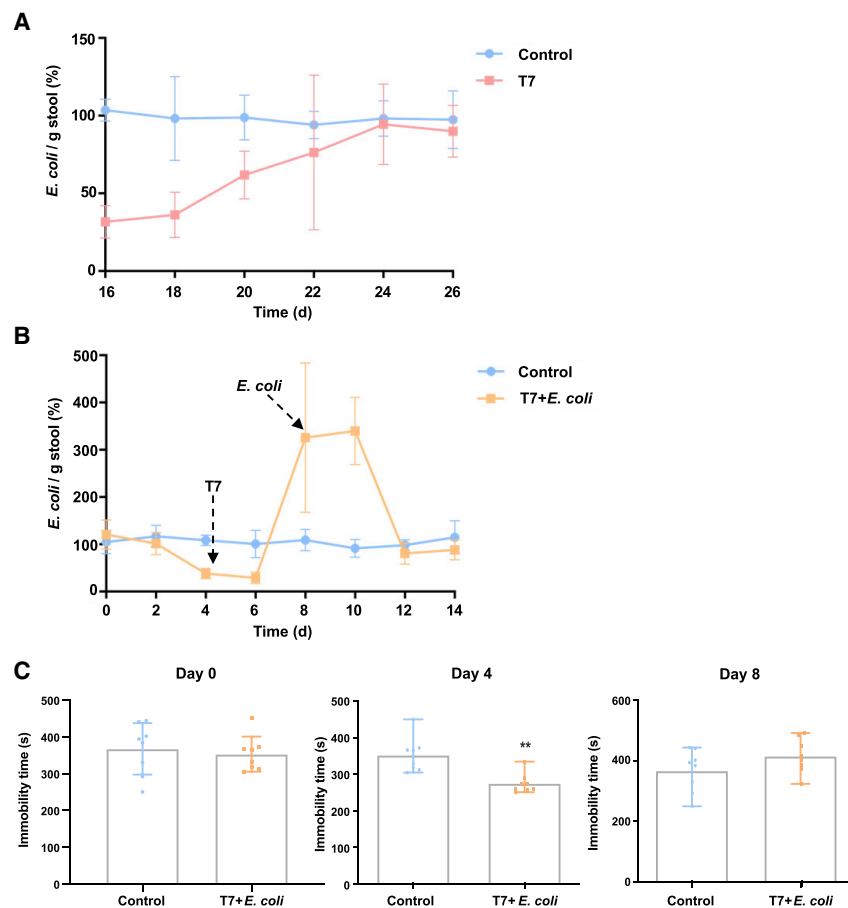


**Figure 5. *E. coli* self-restoration and rescue experiment**

(A) The level of gut *E. coli* in the T7-treated group gradually recovered after the 14 day experiment (data started from day 16) and restored to the pre-phage treatment level at day 24 (n = 12; data displayed as mean ± SD).

(B) The gut *E. coli* level in the T7-treated group during the 14 day rescue experiment with phage administration at day 4 and *E. coli* gavaging at day 8 (n = 12; data displayed as mean ± SD).

(C) TST results at days 0, 4, and 8 showed the correlation between behavioral changes of the mice the depletion and reintroduction of *E. coli* (n = 12; data displayed as mean ± SD).

T7-treated mice (Figure 5B). We treated the experimental group with T7<sup>H</sup> on day 4 and *E. coli* on day 8 and assessed the mouse behavior using the TST on days 0 (baseline), 4 (after T7<sup>H</sup> gavaging), and 8 (after *E. coli* gavaging). The qPCR results revealed a fluctuation in *E. coli* levels due to orally gavaged phage and *E. coli* over the 14 day experiment (Figure 5B). Accordingly, the TST results on the pre-treatment, after T7<sup>H</sup> treated and after *E. coli* rescued, were also reflected in line with the levels of fecal *E. coli* (Figure 5C). To be noted, the result on day 8 suggested that the mice immediately returned to normal after the reintroduction of *E. coli*.

### Conclusion

Germ-free mice and derivations of these models have been widely used in gut microbiota studies to demonstrate the direct link between certain bacteria and human diseases. While this approach provides an advantage to identify the specific contribution of the inoculated microbe in a controlled environment, it does not consider the general microbial population in the community, especially the change in species representation due to a change in one bacterium. Previous studies on *E. coli* using gnotobiotic animals revealed a reinforcement of intestinal defenses along with psychiatric effects. Furthermore, oral administration of *E. coli* has been shown to increase anxiety-like behaviors in healthy mice (Jang et al., 2018), and *E. coli*-derived lipopolysaccharide (LPS) was shown to play an important role

in antidepressant-like, but not anti-anxiety-like, behavior (Luo et al., 2018). Our *E. coli*-depleted TBD model demonstrated the neurological role of *E. coli* in the context of wild-type mice with a complete set of gut microbiota. These mice displayed a unique “brave” behavioral trait, with a degree of resemblance to the previously published behavioral pattern caused by a combined anxiolytic and/or antidepressant treatment (Burokas et al., 2017; Shi et al., 2020; Wang et al., 2019).

By examining the population of *E. coli* and bacterial diversity over time, we conclude that *E. coli* abundance is responsible for the behavior changes observed, and we speculate additional *E. coli*-derived

stimulants may be responsible besides LPS. Being able to quickly assess both the target bacterium and the microbiota environment over time is a clear advantage over the gnotobiotic model, which only examines selected bacteria in isolation. Meanwhile, the potential application of *E. coli* phage as a single dose providing antidepressant or anxiolytic effects to treat depression or anxiety should be investigated further in future studies. This cost-effective and time-efficient TBD model would accelerate the establishment of novel interactions between gut bacteria and health.

### Limitations of the study

While establishing a TBD animal model using a well-known and commercially available phage like T7 is relatively simple, newly isolated phages should be subjected to further characterization to define its host range and potential toxicity. Furthermore, some phages have a rather broad host range that targets bacteria at the genus level, which should be used with caution to avoid collateral depletion of other bacteria. In addition, phage cocktail should be considered to extend the depletion period by reducing the phage resistance, albeit not discussed in this study.

### STAR★METHODS

Detailed methods are provided in the online version of this paper and include the following:



- **KEY RESOURCES TABLE**
- **RESOURCE AVAILABILITY**
  - Lead contact
  - Materials availability
  - Data and code availability
- **EXPERIMENTAL MODEL AND SUBJECT DETAILS**
  - Mice
- **METHOD DETAILS**
  - Phage cultivation and treatment
  - Behavioural tests
  - Open field test (OFT)
  - Elevated plus-maze test (EPM)
  - Novelty-suppressed feeding (NSF) test
  - Tail suspension test (TST)
  - Reciprocal social interaction test (RSIT)
  - Three-chamber sociability test (TCST)
  - Novel object recognition test
  - Quantitative real-time PCR
  - Absolute abundance quantification of gut bacteria
  - Bioinformatic analysis of 16S rRNA amplicon sequencing data
  - Histological analysis and index
- **QUANTIFICATION AND STATISTICAL ANALYSIS**

#### SUPPLEMENTAL INFORMATION

Supplemental information can be found online at <https://doi.org/10.1016/j.crmeth.2022.100324>.

#### ACKNOWLEDGMENTS

We thank Dr. Jing Lin for the figure illusions and Dr. Minhao Liu for useful discussions. This project is supported by the National Key R&D Program of China (2021YFA1301201) and the Key Research and Development Plan of Shaanxi Province (2021ZDLSF01-10).

#### AUTHOR CONTRIBUTIONS

B.L. conceived the study and designed experiments. F.Z., Y.L., Y.W., and X.M. designed the animal experiments. Y.L., S.P., H.W., Z.Y., Z.W., Z.H., and J.Y. performed the research. F.Z. and B.L. analyzed the data. B.L. wrote the first draft paper. Y.L., J.B., and B.L. revised the manuscript with input from all other authors.

#### DECLARATION OF INTERESTS

The authors declare no conflicts of interest.

Received: March 5, 2021  
Revised: August 11, 2022  
Accepted: October 7, 2022  
Published: November 4, 2022

#### REFERENCES

Arumugam, M., Raes, J., Pelletier, E., Le Paslier, D., Yamada, T., Mende, D.R., Fernandes, G.R., Tap, J., Bruls, T., Batto, J.M., et al. (2011). Enterotypes of the human gut microbiome. *Nature* 473, 174–180.

Bolyen, E., Rideout, J.R., Dillon, M.R., Bokulich, N.A., Abnet, C.C., Al-Ghali, G.A., Alexander, H., Alm, E.J., Arumugam, M., Asnicar, F., et al. (2019). Reproducible, interactive, scalable and extensible microbiome data science using QIIME 2. *Nat. Biotechnol.* 37, 852–857.

Burokas, A., Arboleya, S., Moloney, R.D., Peterson, V.L., Murphy, K., Clarke, G., Stanton, C., Dinan, T.G., and Cryan, J.F. (2017). Targeting the microbiota-gut-brain Axis: Prebiotics have anxiolytic and antidepressant-like effects and reverse the impact of chronic stress in mice. *Biol. Psychiatr.* 82, 472–487.

Callahan, B.J., McMurdie, P.J., Rosen, M.J., Han, A.W., Johnson, A.J.A., and Holmes, S.P. (2016). DADA2: high-resolution sample inference from Illumina amplicon data. *Nat. Methods* 13, 581–583.

Carabotti, M., Scirocco, A., Maselli, M.A., and Severi, C. (2015). The gut-brain axis: interactions between enteric microbiota, central and enteric nervous systems. *Ann. Gastroenterol.* 28, 203–209.

Cryan, J.F., Mombereau, C., and Vassout, A. (2005). The tail suspension test as a model for assessing antidepressant activity: Review of pharmacological and genetic studies in mice. *Neurosci. Biobehav. Rev.* 29, 571–625.

Galland, L. (2014). The gut microbiome and the brain. *J. Med. Food* 17, 1261–1272.

Hsu, B.B., Gibson, T.E., Yeliseyev, V., Liu, Q., Lyon, L., Bry, L., Silver, P.A., and Gerber, G.K. (2019). Dynamic modulation of the gut microbiota and Metabolome by bacteriophages in a mouse model. *Cell Host Microbe* 25, 803–814.e5.

Jang, H.M., Lee, K.E., Lee, H.J., and Kim, D.H. (2018). Immobilization stress-induced *Escherichia coli* causes anxiety by inducing NF-kappaB activation through gut microbiota disturbance. *Sci. Rep.* 8, 13897.

Jiang, S.Q., Yu, Y.N., Gao, R.W., Wang, H., Zhang, J., Li, R., Long, X.H., Shen, Q.R., Chen, W., and Cai, F. (2019). High-throughput absolute quantification sequencing reveals the effect of different fertilizer applications on bacterial community in a tomato cultivated coastal saline soil. *Sci. Total Environ.* 687, 601–609.

Kaidanovich-Beilin, O., Lipina, T., Vukobradovic, I., Roder, J., and Woodgett, J.R. (2011). Assessment of social interaction behaviors. *JoVE*, 2473.

Kennedy, E.A., King, K.Y., and Baldrige, M.T. (2018). Mouse microbiota models: comparing germ-free mice and antibiotics treatment as tools for modifying gut bacteria. *Front. Physiol.* 9, 1534.

Kho, Z.Y., and Lal, S.K. (2018). The human gut microbiome - a potential controller of wellness and disease. *Front. Microbiol.* 9, 1835.

Kim, D.G., Gonzales, E.L., Kim, S., Kim, Y., Adil, K.J., Jeon, S.J., Cho, K.S., Kwon, K.J., and Shin, C.Y. (2019). Social interaction test in Home cage as a novel and ethological measure of social behavior in mice. *Exp. Neurobiol.* 28, 247–260.

Kleimann, A., Toto, S., Eberlein, C.K., Kielstein, J.T., Bleich, S., Frieling, H., and Sieberer, M. (2014). Psychiatric symptoms in patients with Shiga toxin-producing *E. coli* O104:H4 induced haemolytic-uraemic syndrome. *PLoS One* 9, e101839.

Knight, D.J.W., and Girling, K.J. (2003). Gut flora in health and disease. *Lancet* 361, 1831.

Lueptow, L.M. (2017). Novel object recognition test for the investigation of learning and memory in mice. *JoVE*.

Luo, Y., Zeng, B., Zeng, L., Du, X., Li, B., Huo, R., Liu, L., Wang, H., Dong, M., Pan, J., et al. (2018). Gut microbiota regulates mouse behaviors through glucocorticoid receptor pathway genes in the hippocampus. *Transl. Psychiatry* 8, 187.

Matarazzo, I., Toniato, E., and Robuffo, I. (2018). Psychobiome feeding Mind: Polyphenolics in depression and anxiety. *Curr. Top. Med. Chem.* 18, 2108–2115.

Petra, A.I., Panagiotidou, S., Hatzigelaki, E., Stewart, J.M., Conti, P., and Theoharides, T.C. (2015). Gut-microbiota-brain Axis and its effect on neuropsychiatric Disorders with suspected immune dysregulation. *Clin. Therapeut.* 37, 984–995.

Quigley, E.M.M. (2013). Gut bacteria in health and disease. *Gastroenterol. Hepatol.* 9, 560–569.

Ramaker, M.J., and Dulawa, S.C. (2017). Identifying fast-onset antidepressants using rodent models. *Mol. Psychiatr.* 22, 656–665.

Seibenhener, M.L., and Wooten, M.C. (2015). Use of the Open Field Maze to measure locomotor and anxiety-like behavior in mice. *JoVE*, e52434.

- Sender, R., Fuchs, S., and Milo, R. (2016). Revised estimates for the number of human and bacteria cells in the body. *PLoS Biol.* *14*, e1002533.
- Shi, X., Gao, Y., Song, L., Zhao, P., Zhang, Y., Ding, Y., Sun, R., Du, Y., Gong, M., Gao, Q., et al. (2020). Sulfur dioxide derivatives produce antidepressant- and anxiolytic-like effects in mice. *Neuropharmacology* *176*, 108252.
- Stephens, M.A.C., and Wand, G. (2012). Stress and the HPA axis: role of glucocorticoids in alcohol dependence. *Alcohol Res.* *34*, 468–483.
- Umesaki, Y. (2014). Use of gnotobiotic mice to identify and characterize key microbes responsible for the development of the intestinal immune system. *Proc. Jpn. Acad. Ser. B Phys. Biol. Sci.* *90*, 313–332.
- Valles-Colomer, M., Falony, G., Darzi, Y., Tigchelaar, E.F., Wang, J., Tito, R.Y., Schiweck, C., Kurilshikov, A., Joossens, M., Wijnemga, C., et al. (2019). The neuroactive potential of the human gut microbiota in quality of life and depression. *Nat. Microbiol.* *4*, 623–632.
- Visconti, A., Le Roy, C.I., Rosa, F., Rossi, N., Martin, T.C., Mohney, R.P., Li, W., de Rinaldis, E., Bell, J.T., Venter, J.C., et al. (2019). Interplay between the human gut microbiome and host metabolism. *Nat. Commun.* *10*, 4505.
- Walf, A.A., and Frye, C.A. (2007). The use of the elevated plus maze as an assay of anxiety-related behavior in rodents. *Nat. Protoc.* *2*, 322–328.
- Walsh, J., Griffin, B.T., Clarke, G., and Hyland, N.P. (2018). Drug-gut microbiota interactions: implications for neuropharmacology. *Br. J. Pharmacol.* *175*, 4415–4429.
- Wang, X., Xiu, Z., Du, Y., Li, Y., Yang, J., Gao, Y., Li, F., Yin, X., and Shi, H. (2019). Brazilin treatment produces antidepressant- and anxiolytic-like effects in mice. *Biol. Pharm. Bull.* *42*, 1268–1274.
- Weersma, R.K., Zhernakova, A., and Fu, J. (2020). Interaction between drugs and the gut microbiome. *Gut* *69*, 1510–1519.
- Zhu, F., Ju, Y., Wang, W., Wang, Q., Guo, R., Ma, Q., Sun, Q., Fan, Y., Xie, Y., Yang, Z., et al. (2020). Metagenome-wide association of gut microbiome features for schizophrenia. *Nat. Commun.* *11*, 1612.
- Zitvogel, L., Galluzzi, L., Viaud, S., Vétizou, M., Daillère, R., Merad, M., and Kroemer, G. (2015). Cancer and the gut microbiota: an unexpected link. *Sci. Transl. Med.* *7*, 271ps1.

## STAR★METHODS

### KEY RESOURCES TABLE

REAGENT or RESOURCE	SOURCE	IDENTIFIER
<b>Chemicals, peptides, and recombinant proteins</b>		
NaHCO <sub>3</sub>	Aladdin	Cat#S5761
Tryptone	Aladdin	Cat#T139519
Yeast extract	Beyotime	Cat#ST968
LB medium	AOBOX	Cat#02-136-y250g
Ethanol	Merck	Cat#E7023
Neutral Paraformaldehyde Fixative	Servicebio	Cat#G1101
Hematoxylin	Servicebio	Cat#G1039
Eosin	Servicebio	Cat#G1005
<b>Critical commercial assays</b>		
QIAamp Fast DNA Stool Mini Kit	Qiagen	Cat#51604
Supplemental Microbial qpcr Mastermix(Rox)	Qiagen	Cat#330530
FastDNA Spin Kit for Soil	MP Biomedicals	Cat#116560200
<b>Experimental models: Organisms/strains</b>		
Mouse: WT C57BL/6J	Experimental Animal Centre of Xi'an Jiaotong University	N/A
<i>E. coli</i> TOP10 Competent Cells	Biomed	Cat#BC102-02
<i>Escherichia coli</i> bacteriophage T7	ATCC	Cat#BAA-1025-B2
<b>Recombinant DNA</b>		
Plasmid pUC57- <i>E. coli</i>	This paper	N/A
Plasmid pUC57- total	This paper	N/A
<b>Software and algorithms</b>		
SMART 3.0	Panlab	<a href="https://www.panlab.com/">https://www.panlab.com/</a>
GraphPad Prism 9	GraphPad Software, Inc.	<a href="https://www.graphpad.com/">https://www.graphpad.com/</a>
QIIME 2	QIIME 2 development team	<a href="https://www.qiime.org">https://www.qiime.org</a>
DADA 2	Benjamin Callahan	<a href="https://www.benjineb.github.io">https://www.benjineb.github.io</a>
Greengenes	Second Genome,inc	<a href="http://Greengenes.secondgenome.com">Greengenes.secondgenome.com</a>
CFX Maestro Software	Bio-Rad	<a href="https://www.bio-rad.com/">https://www.bio-rad.com/</a>
GRYPHAX Software	JENOPTIK	<a href="https://www.jenoptik.com/">https://www.jenoptik.com/</a>
<b>Other</b>		
0.22 μm filter	Millipore	Cat#SLGPR33RB
Nanodrop 2000	Thermo Fisher	N/A
Quibit 3.0	Thermo Fisher	N/A
NovaSeq 6000 System	Illumina,inc	N/A
CFX Connect Real-Time PCR Detection System	Bio-Rad	Cat#1855201
Axio Zoom.V16 for Biology	Zeiss	N/A

### RESOURCE AVAILABILITY

#### Lead contact

Further information and requests for resources and reagents should be directed to and will be fulfilled by the lead contact, Bing Liu ([bliu2018@xjtu.edu.cn](mailto:bliu2018@xjtu.edu.cn)).

### Materials availability

This study did not generate new unique reagents.

### Data and code availability

- All the data published in this paper will be available from the [lead contact](#) upon request.
- No original codes were used in this paper.
- Any additional information required to reanalyze the data reported in this paper is available from the [lead contact](#) upon request.

## EXPERIMENTAL MODEL AND SUBJECT DETAILS

### Mice

Each group contains 12 healthy 6-week-old female C57BL/6J mice which were purchased from the Experimental Animal Centre of Xi'an Jiaotong University and housed in the animal facility with standard chow and autoclaved water and maintained under a 12-h light/dark cycle. Ethical approval was granted by the laboratory animal care committee of Xi'an Jiaotong University with approval number: XJTULAC2019-1276.

## METHOD DETAILS

### Phage cultivation and treatment

*Escherichia coli* phage T7 (obtained from ATCC) was incubated with *E. coli* (strain K12) culture at OD<sub>600</sub> 0.4 at 37°C with shaking until the solution became clear. The lysates were centrifuged at 4,000 × g for 30 min to remove the remaining bacterial cells and debris, and then supernatant was filtered using a 0.2 μm membrane filter and kept at 4°C. The bacteriophage titer was measured using the double-layer plate method and diluted to the required titer. Mice were orally administrated with NaHCO<sub>3</sub> to neutralize gastric acid prior to phage treatment, followed by gavaging water, deactivated 1 × 10<sup>11</sup> T7, 1 × 10<sup>6</sup> T7 and 1 × 10<sup>11</sup> T7, respectively. Fecal samples were collected at day 0, 1, 2, 4, 6, 8, 10, 12 and 14 after phage treatment.

### Behavioural tests

The behavioural tests consisted of multiple experiments outlined below:

#### Open field test (OFT)

All mice were housed in the testing room for acclimation at least 1 h before behavioural testing. The animal was placed individually in the centre of the device that was constructed from an opaque black box (45 × 45 × 45 cm) and allowed to explore freely for 30 min. The total distance travelled and the time spent in the central zone (15 × 15 cm) were recorded and analysed using the SMART 3.0 software. After each mouse was tested, 75% ethanol was used to clean faeces and eliminate odour.

#### Elevated plus-maze test (EPM)

The maze consisted of two open arms (50 × 10 × 1 cm) and two closed arms (50 × 10 × 40 cm) arranged such that two open arms were opposite to each other, located 50 cm above the floor. The animals were placed in the central square (10 × 10 cm) of the plus-shaped maze, facing one of the open arms, and were allowed to explore the whole maze for 8 min. The time spent in each arm and number of entries through the open and closed arms were manually counted by examining filmed video. The ratios of open arm/total entries and total time were accepted as indexes of anxiety in mice. After each mouse was tested, 75% ethanol was used to clean faeces and eliminate odour.

#### Novelty-suppressed feeding (NSF) test

All mice were food-deprived for 24 h prior to the test. Then each mouse was placed in an illuminated and soundproofed box (45 × 45 × 45 cm) covered with wooden bedding, a piece of paper was placed in the center of the field, on a white paper that contained a small piece of mouse chow. The time until the first feeding episode was recorded as the latency and food consumption during the subsequent 5 min was measured to eliminate the effect of appetite on the latency time.

#### Tail suspension test (TST)

Each mouse was suspended using adhesive tape to a tail-suspension box for 6 min, in such a position that it could not escape or hold on to nearby surfaces. The time of immobility was manually counted by examining filmed video. After each mouse was tested, 75% ethanol was used to clean faeces and eliminate odour.

#### Reciprocal social interaction test (RSIT)

Two subject mice were placed in an opaque black box (45 × 45 × 45 cm), from different cages in the same group, and the social behavior of subject mice was recorded by an overhead camera for 30 min. The total time a pair of mice engaged in social interaction,

including touching, nose-to-nose sniffing, close following, nose-to-anus sniffing, and crawling over/under each other, was manually counted by examining recorded video. After each mouse was tested, 75% ethanol was used to clean faeces and eliminate odour.

### Three-chamber sociability test (TCST)

The testing apparatus used was a rectangular three-chamber box, with two lateral chambers connected to a central chamber, and each lateral chamber contained a small Plexiglas cylindrical cage. Each subject mouse was placed in the central chamber and allowed to freely explore for 5 min. Then a new mouse was confined in a round, wire cup located in one chamber of the apparatus, while the cup in the other chamber was left empty. During the sociability phase, the test mouse was allowed to freely explore all three chambers for 10 min, the time spent in each cup (touching, sniffing) was recorded by a video camera. In the last 10 min, another new mouse was transferred to the other side of the cup, in the same manner, the time spent in each cup (touching, sniffing) was recorded by a video camera. The percent of time spent in the first mouse and second mouse were used to evaluate the sociability and social novelty. After each mouse was tested, 75% ethanol was used to clean faeces and eliminate odour.

### Novel object recognition test

The experimental mice were transferred to the opaque black box as described in the open field test, and given 10 min to investigate two familiar objects that were placed at adjacent edges of the central area of the box. After 1 h, the test mice were re-exposed to one of the familiar objects together with a novel object for 5 min. The time of exploratory (touching, sniffing and licking the object) directed at each object was recorded by a video camera. Discrimination index (DI) was calculated as a measure of memory, which is the ratio of time spent exploring the novel object to the total time spent exploring both objects. After 24 h, the same recognition was carried to assess long-term memory. After each mouse was tested, 75% ethanol was used to clean faeces and eliminate odour, and the objects were also cleaned with 75% ethanol between each trial.

### Quantitative real-time PCR

Total bacterial and *E. coli* populations in the faeces of mice were quantified by qPCR of the 16S rRNA gene in one mass unit of fecal DNA. Mice fecal DNA was extracted using QIA<sup>®</sup>amp DNA Stool Mini Kit following the manufacturer's instructions. Primers were designed to complement the conserved fragment of bacterial and *E. coli* 16S rRNA gene. The sequences of primer are as follows: total bacterial forward primer (5'-AAACTCAAAGGAATTGACGG-3'), total bacterial reverse primer (5'-CTCACRRACGAGCTGAC-3'), *E. coli* forward primer (5'-GAGCGCAACCCCTTATCCTTTG-3'), *E. coli* reverse primer (5'-TACTAGCGATTCCGACTTCATGG). PUC57 vector was used as the *E. coli* or bacterial standard plasmid by inserting corresponding conservative sequences and a standard curve was plotted using a series of standard plasmid at various concentrations. The absolute copy number of 16S rRNA gene in each mice fecal DNA was calculated by comparison with the standard curve and copy number in a fecal sample was normalized by its total DNA mass.

T7 phage populations in the faeces of mice were quantified by qPCR of the genome in one mass unit of fecal DNA. Primers were designed to complement the conserved fragment of T7 phage genome. The sequences of primer are as follows: T7 phage forward primer (5'- CCTCTTGGGAGGAAGAGATTTG -3'), T7 phage reverse primer (5'- TACGGGTCTCGTAGGACTTAAT -3'). T7 phage genome at various concentrations were used to plot a standard curve. The absolute copy number of T7 phage gene in each mice fecal DNA was calculated by comparison with the standard curve and copy number in a fecal sample was normalized by its total DNA mass.

### Absolute abundance quantification of gut bacteria

Absolute abundance quantification of 16S rRNA amplicon sequencing was performed by Genesky Biotechnologies Inc., Shanghai, 201315 (China). Briefly, total genomic DNA was extracted from feces using the FastDNA<sup>®</sup> SPIN Kit for Soil (MP Biomedicals, Santa Ana, CA) according to the manufacturer's instructions. The integrity of genomic DNA was detected through agarose gel electrophoresis. The concentration and purity of genomic DNA were measured through the Nanodrop 2000 and Qubit3.0 Spectrophotometer, respectively. Artificially synthesized multiple spike-in sequences were added to the sample DNA with known gradient copy numbers, acting as the reference genes to calculate the absolute abundance of test bacteria. The multiple spike-ins had identical conserved regions to complement natural 16S rRNA genes but their variable regions were replaced by random sequence with ~40% GC content. The V3-V4 hypervariable regions of the 16S rRNA gene of test bacteria and spike-ins were amplified with the primers 341F (5'-CCTACGGGNGGCWGCAG-3') and 805R (5'-GACTACHVGGGTATCTAATCC-3') and then sequenced using Illumina NovaSeq 6000 sequencer.

### Bioinformatic analysis of 16S rRNA amplicon sequencing data

All processing and analysis of raw read sequences were conducted in an integrative tool of microbiome data, QIIME2 (Bolyen et al., 2019). The adaptor and primer sequences were trimmed using the cutadapt plugin. Quality control of raw reads and identification of amplicon sequence variants (ASVs) were fulfilled in DADA2 plugin (Callahan et al., 2016). ASV representative sequence was assigned to a given taxonomy at the confidence threshold of 0.8 by a pre-trained Naive Bayes classifier which was trained on the Greengenes (version 13.8). Then read numbers of the spike-in sequences and ASVs were counted. Standard curves and regression equations for each sample were established via linear regression which used read counts as the independent variable and spike-in copy number as



the dependent variable. The absolute copy number of each ASV in each sample was calculated using the regression equation, in which the read counts of the corresponding ASV were input as the independent variable. The spike-in sequence needs to be removed in the subsequent analysis (Jiang et al., 2019), such as using alpha and beta diversity calculation.

### **Histological analysis and index**

After the behavioural experiments, three random mice in each group were cardiac perfused with 4% paraformaldehyde to obtain the heart, liver, spleen, lung, kidney, brain, intestine and brain, all obtained tissues were fixed in paraformaldehyde and embedded in paraffin. Formalin-fixed paraffin-embedded tissues were sectioned and stained with haematoxylin and eosin using conventional methods.

### **QUANTIFICATION AND STATISTICAL ANALYSIS**

Statistical analysis for individual experiments is indicated as described in figure legends. Statistical significance was determined using a two-tailed t-test when only two groups were analyzed unless specifically noted. \* $p < 0.05$ , \*\* $p < 0.005$ , \*\*\* $p < 0.0005$ . All results were statistical analyzed by GraphPad Prism and Excel.